

Self-rotation of optical polarization in rubidium vapor

Shuwei Qiu (邱淑伟)¹, Wenge Guo (郭文阁)^{1*}, Mingtao Cao (曹明涛)², Tao Liu (刘 韬)²,
Liang Han (韩 亮)², Hao Liu (刘 昊)², Pei Zhang (张 沛)², Shougang Zhang (张首刚)³,
Hong Gao (高 宏)^{2**}, and Fuli Li (李福利)²

¹MOE Key Laboratory for Electricity Gas and Oil Logging, Xi'an Shiyu University, Xi'an 710065, China

²MOE Key Laboratory for Nonequilibrium Synthesis and Modulation of Condensed Matter,
Xi'an Jiaotong University, Xi'an 710049, China

³CAS Key Lab Time & Frequency Primary Standard, National Time Service Center, Xi'an 710600, China

*Corresponding author: wguo@xsyu.edu.cn; **corresponding author: honggao@mail.xjtu.edu.cn

Received September 6, 2011; accepted November 22, 2011; posted online January 18, 2012

We present an experimental and theoretical study of self-rotation of optical polarization in a rubidium vapor. The atomic vapor is placed in a magnetic shielding cavity to suppress the Faraday rotation effect. In our experiment, Doppler-free spectroscopy configuration is used, and $F = 2 \rightarrow F' = 3$ transition of ^{87}Rb D2 line is chosen. We observe self-rotation of optical polarization effect at different pump light ellipticities. A theoretical analysis is then provided based on the experimental conditions. Theoretical simulation and experimental results are in good agreement.

OCIS codes: 270.0270, 020.0020.

doi: 10.3788/COL201210.052701.

When an elliptically polarized light interacts with atoms in the vicinity of resonance, the elliptically polarized plane of the light can rotate. This so-called self-rotation of optical polarization effect was first observed in molecular liquids^[1,2]. This effect is caused by Kerr nonlinearity in solids and liquids^[3]. In atomic vapor, it is caused by optical pumping and AC-Stack shifts^[4]. Unlike the Faraday rotation effect, self-rotation of optical polarization does not require an additional magnetic field. Its dramatic feature is that the optical polarization rotation angle depends on the light ellipticity. If an external magnetic field is present, self-rotation of optical polarization is superimposed on other effects, such as the Faraday rotation effect. The self-rotation of optical polarization can be used for the measurement of Kerr nonlinearities in mediums. It is a useful diagnostic tool for the experiments on photon-photon interactions or photon-condensed matter in atomic media, and provides a method of detecting a weak magnetic field^[2]. It also leads to the squeezed states of light in which the quantum noise fluctuations drop below the standard quantum limit^[3-7]. Moreover, a recent study has shown that polarization self-rotation provides a feasible way for laser frequency stabilization without any modulation and magnetic field^[8].

Self-rotation of optical polarization effect can be understood as follows. The polarization of a classical monochromatic light is described by two circularly polarized components: σ_R (right-hand polarization) and σ_L (left-hand polarization). Both components have certain relative phases and amplitudes for a determinate polarized light. If a polarized light enters the atomic vapor and interacts with an atomic transition in the vicinity of resonance, the two polarization components of light couples with the different Zeeman sublevels. If the intensities of the two components are unequal, the populations of the Zeeman sublevels become different via optical

pumping. As a result, the atom sample refractive index is different for the two circular polarization components, which causes the polarized plane of the incident light to rotate.

Self-rotation of optical polarization has been studied extensively both theoretically and experimentally for an atomic assemble. However, extant studies either focus on the complex experimental phenomena and theoretical simulation with multiple transitions^[3] or treat the self-rotation of optical polarization with Faraday rotation and absorption also taken into account^[1,2,7,8]. In this letter, we report the self-rotation of optical polarization in a rubidium vapor. Compared with other studies, two kinds of situation are specifically considered. Firstly, the atom vapor is placed in a shielding cavity to avoid the earth magnetic field, so that Faraday rotation effect can be eliminated as much as possible. Secondly, saturated absorption configuration is used to reduce the light absorption when working close to the atomic resonant. Through this method, we can provide a direct study on the effect of self-rotation of optical polarization. In our experiment, we also choose the $F = 2 \rightarrow F' = 3$ transition of ^{87}Rb D2 line because this transition is well isolated from other lines and is directly accessible to theoretical analysis. We observe the self-rotation angle of optical polarization at different pump light ellipticities. Then, a simple physical model is built to analyze our experimental results. Theoretical simulation and experiment results are in good agreement.

The diagram of the experimental arrangement is shown in Fig.1, which is similar to that reported in Ref. [8]. In our experiment, we use an external cavity diode laser operating at 780 nm with single-mode output in the vicinity of ^{87}Rb D2 line ($F = 2 \rightarrow F' = 3$) transition. The external cavity diode laser can be roughly tuned by manually adjusting the grating, and subsequently finely tuned by applying a certain voltage to the PZT attached to

the grating. A monochromatic light from the laser is split into two equal parts by a 50/50 beam splitter. The transmitted beam is used as the reference light, whereas the reflected light is used as the experimental light. The reference light is used for the ^{87}Rb saturated absorption experiment to monitor the laser frequency. The experimental light is for our main experiment to detect the polarization rotation. This part of the light passes through the PBS (polarized beam splitter) to yield two orthogonal polarized beams. The output beam parallel to the horizontal plane, called the p-polarized beam, is used as probe beam. The output beam orthogonal to the horizontal plane, called the s-polarized beam, is used as pump light. The intensity ratio of probe and pump light is controlled by a half-wave plate before the PBS to be approximately, $I_{\text{probe}}/I_{\text{pump}} = 0.01$. A quarter-wave plate is placed on the way of the pump light before it enters the atom vapor cell. The polarization of the pump light is thus changed by rotating the orientation angle of the fast axis of the quarter-wave plate with respect to the horizontal axis. The atomic vapor is placed in a magnetic shielding cavity. The shielding cavity contains three layers to ensure that the strength of earth magnetic field is as small as possible in the region where the atom vapor is placed^[9]. In our setup, the residual earth magnetic field is detected below Gauss meter resolution (~ 2 mG). Thus, the influence of Faraday rotation effect can be eliminated as much as possible. Length of the atomic vapor cells is 100 mm and cell diameter is 25 mm. At room temperature, the density of rubidium vapor cell is approximately $3 \times 10^{12} \text{ cm}^{-3}$.

Because Doppler broadening is usually the main obstacle in observing the hyperfine structure of atomic spectrum, in our experiment, we use the saturated absorption spectroscopy technique^[10]. Doppler-free saturated absorption spectrum measurement also provides an optical pumping effect to reduce the absorption when the probe light is used near the resonance. The pump and probe beam pass through the atom vapor in opposite directions, and the two beams cross each other with a small inclined angle in order to reach a larger overlap. The beam diameters of the pump and probe beam in the center of the rubidium vapor cell are approximately 3 and 1 mm, respectively. Doppler broadening can be eliminated in the overlapping region of the two beams. The probe beam exiting the cell then passes through the combination of a half-wave plate and a PBS composed of a balanced polarimeter set for detection of the light-induced rotation of the polarization plane. The probe beam is then decomposed into two orthogonally polarized beams, which are detected by two detectors (D_x and D_y). Figure 2 shows the rubidium-saturated absorption spectrum of the D2 lines. The transition $F = 2 \rightarrow F' = 3$ is selected for the following self-rotation of optical polarization experiment because this line is clearly isolated from other lines and is convenient for the theoretical analysis.

Figure 3 shows the self-rotation angle of optical polarization as a function of the laser detuning and pumping light ellipticities. An apparent relation clearly exists between the quarter-wave plate orientation angle and the self-rotation angle of optical polarization. In Fig. 3, curve (a) corresponds to the linear polarization of the pump light. Clearly, the linearly polarized pump light

almost causes no rotation. The small slope may be due to the residual magnetic field. Curves (b) and (c) correspond to the cases when the pump light turns to be elliptically polarized by rotating the quarter-wave plate orientation angles of $\theta = 20^\circ$ and 30° , respectively. Curve (d) corresponds to the case that the pump beam is circularly polarized, which means the orientation angle of the quarter-wave plate is $\theta = 45^\circ$. The figure shows that the self-rotation angle of optical polarization of the probe beam changes more and more dramatically as the polarization of the pump beam varies from linearly polarized to elliptically polarized. This trend reaches the maximum when the pump light turns to be circularly polarized; the largest optical polarization rotated angle in our experiment is $\varphi \approx 0.07$ rad.

Based on our experimental configuration and results, we provide a theoretical simulation. The above atomic transition is a simplified V-type three-level atomic structure, as shown in Fig. 4. The two upper levels $m_{F'} = -1$ and $m_{F'} = 1$ are coupled with a single lower level m_F through the left circular polarized light σ_L and the right circular polarized light σ_R , respectively. Because the pump light power is much higher than that of probe beam, the pump light can be used as the prepopulation for the corresponding sublevels. Linearly polarized pump light generates a symmetric population on each arm, whereas an elliptically or circularly polarized pump light causes an asymmetric population. A weak probe beam propagating through such system has less effect on the population created by the pump light, but suffers from the different index of refraction for each arm due to

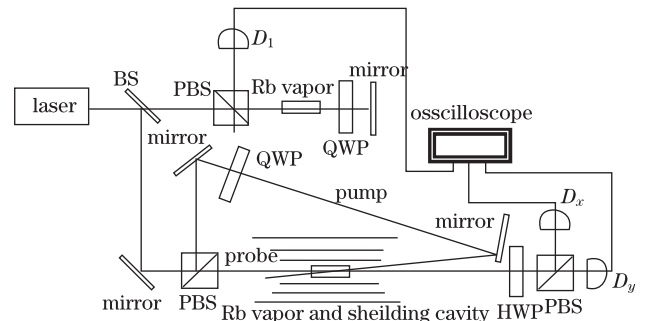


Fig. 1. Schematic configuration of our experiment. D_1 , D_x and D_y : photodetectors; BS: beam splitter; PBS: polarized beam splitter; QWP: quarter-wave plate; HWP: half wave plate.

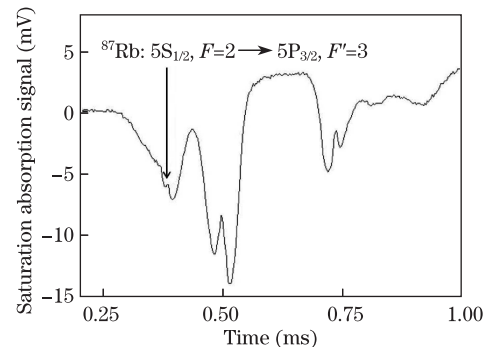


Fig. 2. Measured rubidium-saturated absorption spectra of D2 lines. The arrow points out the transition line used in the experiment.

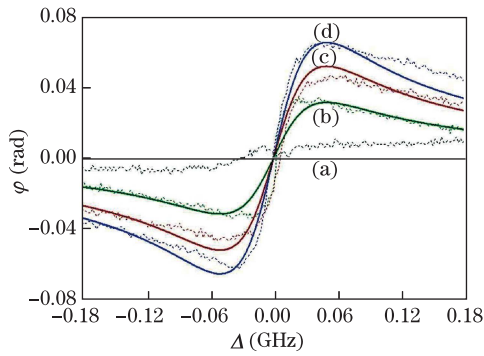


Fig. 3. Measured (dotted lines) and numerical simulation (solid lines) results of optical polarization rotated angles as a function of the laser detuning at different pump-light ellipticities. The different polarization of pump light can be generated by rotating QWP orientation angle θ : (a) $\theta = 0^\circ$ (linearly polarized light); (b), (c) $\theta = 20^\circ$ and 30° (elliptically polarized light); (d) $\theta = 45^\circ$ (circularly polarized light).

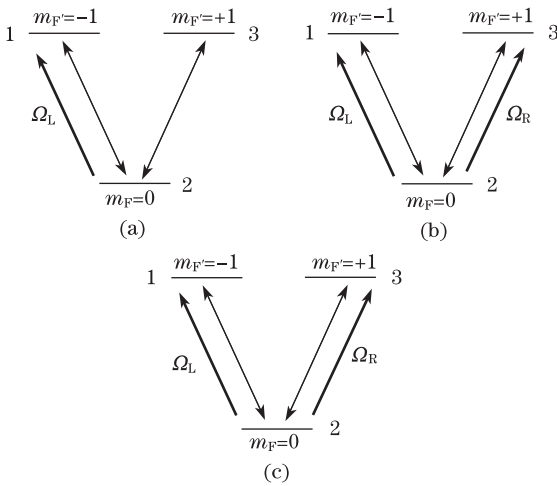


Fig. 4. Simplified atomic three-level scheme for the different pump-light polarization states (thick arrow lines). The probe beam is linearly polarized (thin arrow lines): (a) circularly polarized ($\Omega_L \neq 0, \Omega_R = 0$); (b) elliptically polarized ($\Omega_L \neq \Omega_R$); (c) linearly polarized ($\Omega_L = \Omega_R$). Here, Ω_R and Ω_L denote the Rabi frequency of right and left circularly polarized pump light, respectively.

different populations. The individual population of the three levels caused by the pump light can be estimated by^[11]

$$\begin{aligned} \dot{\rho}_- &= \Omega_L(\rho - \rho_-) - \Gamma\rho_-, \\ \dot{\rho}_+ &= \Omega_R(\rho - \rho_+) - \Gamma\rho_+, \\ \dot{\rho} &= \Omega_R(\rho_+ - \rho) + \Omega_L(\rho_- - \rho) + \Gamma(\rho_+ + \rho_-), \end{aligned} \quad (1)$$

where Ω_R and Ω_L are the Rabi frequency of the right and left circularly polarized components of the pump light, respectively; ρ , ρ_+ , and ρ_- are the atomic relative population of $m_F = 0$ and $m_{F'} = \pm 1$; and Γ is the natural line width of the upper level. To solve the equations, we assume the initial conditions are $\rho_- = \rho_+ = 0.0$ and $\rho = 1.0$. The Rabi frequency Ω_R and Ω_L can be related with the orientation angle θ of the quarter-wave plate with $\Omega_R \propto \sin^2(45^\circ - \theta)$ and $\Omega_L \propto \cos^2(45^\circ - \theta)$. Therefore, we can simulate the self-rotation of optical polarization according to Ω_R and Ω_L by changing the orientation

angle of the quarter-wave plate.

Equation (1) is numerically solved by allowing the relative population to approach steady state. Thus, the refractive index of atom vapor $n(\omega)$ experienced by the weak probe beam can be described as

$$\begin{aligned} n_R(\omega) &= 1 + \frac{e^2}{2m\varepsilon_0\omega_0} \cdot \frac{\rho_+ - \rho}{2(\omega - \omega_0) + i\Gamma}, \\ n_L(\omega) &= 1 + \frac{e^2}{2m\varepsilon_0\omega_0} \cdot \frac{\rho_- - \rho}{2(\omega - \omega_0) + i\Gamma}, \end{aligned} \quad (2)$$

where e is the unit electricity quantity of a charge, m is the unit mass of a charge, ε_0 is the vacuum dielectric constant, ω_0 is the atomic resonance frequency, and ω is the laser frequency. After the probe beam propagates through the atomic vapor, the two circular components of probe beam acquire a relative phase shift of

$$\Phi = \frac{\omega\ell}{c} \cdot \text{Re}[n_R(\omega) - n_L(\omega)], \quad (3)$$

where ℓ is the path length in the vapor and c is the light vacuum speed. Therefore, the rotation angle of the polarized plane of the probe beam can be described as $\varphi = \Phi/2$. Finally, we can use our expression for optical-pumping-induced difference in the refractive indices for σ_R and σ_L probe beam to determine the dependence of self-rotation of optical polarization for different laser frequency detuning, $\Delta = \omega - \omega_0$,

$$\varphi = K \cdot (\rho_+ - \rho_-) \cdot \frac{\Delta \cdot \left(\Delta^2 - \frac{\Gamma^2}{4} \right) + \Delta \cdot \frac{\Gamma^2}{2}}{\left(\Delta^2 - \frac{\Gamma^2}{4} \right)^2 + \Gamma^2 \cdot \Delta^2}, \quad (4)$$

where $K = \omega\ell e^2/8m\varepsilon_0\omega_0$. The solid lines in Fig. 3 show the numerical simulation results. The theoretical results are scaled down to fit the experimental results. The figure shows that the variation tendency of theoretical results agrees well with the experimental results.

In conclusion, self-rotation of optical polarization has been studied experimentally and theoretically in an atomic vapor. Both experimental results and theoretical analysis show that self-rotation of optical polarization is related to the ellipticity of pump light. Self-rotation of optical polarization could be applied to detect weak magnetic field and generate a squeezed vacuum. The spectrum of self-rotation of optical polarization can also be used for the laser-frequency stabilization in absence of any modulation and magnetic field.

This work was supported by the National Natural Science Foundation of China (Nos. 11074198 and 10834007), the Special Prophase Project on the National Basic Research Program of China (No. 2011CB311807), the NSF for Distinguished Young Scholars of China (No. 61025023), and the Scientific Special Project of Shaanxi Province (Nos. 2011JM8028 and 11JK0768).

References

1. I. Novikova, A. B. Matsko, and G. R. Welch, *J. Mod. Opt.* **49**, 2565 (2002).
2. S. M. Rochester, D. S. Hsiung, D. Budker, R. Y. Chiao, D. F. Kimball, and V. V. Yashchuk, *Phys. Rev. A* **63**, 043814 (2001).

3. W. V. Davis, A. L. Gaeta, and R. W. Boyd, *Opt. Lett.* **17**, 18 (1992).
4. M. Fleischhauer, A. B. Matako, and M. O. Scully, *Phys. Rev. A* **62**, 013808 (2000).
5. I. Novikova, A. B. Matsko, V. A. Sautenkov, V. L. Velichansky, G. R. Welch, and M. O. Scully, *Opt. Lett.* **25**, 1651 (2000).
6. E. E. Mikhailov, A. Lezam, T. W. Noel, and I. Novikova, *J. Mod. Opt.* **56**, 1985 (2009).
7. T. Horrom, S. Balik, A. Lezama, M. D. Havey, and E. E. Mikhailov, *Phys. Rev. A* **83**, 053850 (2011).
8. L. Krzemien, K. Brzozowski, A. Noga, M. Witkowski, J. Zachorowski, M. Zawada, and W. Gawlik, *Opt. Commun.* **284**, 1247 (2011).
9. C. Shi, R. Wei, Z. Zhou, D. Lu, T. Li, and Y. Wang, *Chin. Opt. Lett.* **8**, 549 (2010).
10. C. J. Foot, *Atomic Physics* (Oxford University Press, England, 2005).
11. Y. Qi, H. Gao, and S. Zhang, *Chin. Opt. Lett.* **8**, 1 (2010).